

# Magnetic multipole analysis of kagomé and artificial ice dipolar arrays

Gunnar Möller<sup>1</sup> and Roderich Moessner<sup>2</sup>

<sup>1</sup> TCM Group, Cavendish Laboratory, J. J. Thomson Ave., Cambridge CB3 0HE, UK

<sup>2</sup> Max Planck Institute for the Physics of Complex Systems, Dresden, Germany

(Dated: June 25, 2009)

We analyse an array of linearly extended monodomain dipoles forming square and kagomé lattices. We find that its phase diagram contains two (distinct) finite-entropy kagomé ice regimes—one disordered, one algebraic—as well as a low-temperature ordered phase. In the limit of the islands almost touching, we find a staircase of corresponding entropy plateaux, which is analytically captured by a theory based on magnetic charges. For the case of a modified square ice array, we show that the charges ('monopoles') are excitations experiencing two distinct Coulomb interactions: a magnetic 'three-dimensional' one as well as a logarithmic 'two dimensional' one of entropic origin.

An intensifying experimental effort is under way aimed at constructing dipolar arrays of monodomain nanomagnets.<sup>1–4</sup> From a technological viewpoint, this is a promising approach as it harnesses mature techniques—for example those involved in the lithographic preparation of arrays—often highly developed in an industrial context. Indeed, one of the fundamental questions from this perspective is to understand interactions and dynamics of closely packed nanomagnets as these are among the factors determining performance limits on high-density magnetic storage media.

From a many-body physics angle, this forms one aspect of a wider program of studying artificial systems which can be constructed, manipulated and probed on the level of an individual degree of freedom. Pioneering experiments by Wang *et al.* on the two-dimensional 'square ice' array have established a proof-of-principle of the feasibility of such an enterprise<sup>1</sup> by demonstrating that the magnets assume configurations reflecting their interactions, paving the way to a study of their collective properties.<sup>1,5</sup>

While the study of dipolar magnets is a rich subject with a venerable tradition<sup>6</sup> with a recently rejuvenated activity in the context of cold gases<sup>7</sup>—interesting on account of the long ranged and anisotropic nature of the interactions—recent work on the spin ice compounds<sup>8</sup> has found a number of surprising new phenomena. In particular, it was found that even the complex dipolar interactions can lead to large low-temperature degeneracies, apparently with little additional fine-tuning.<sup>9–11</sup> A simple model which considered each magnetic dipole as a pair of nearly opposite magnetic charges ("monopoles") was able to account for this phenomenon analytically, and established that in spin ice, these monopoles are the appropriate degrees of freedom at low temperatures.<sup>12</sup>

In this paper, we analyse interactions in artificial dipolar arrays in  $d = 2$ . We study two geometries, the qualitative behavior of which varies reflecting simple lattice parameters such as even/oddness of their coordination. Besides the abovementioned artificial spin ice, we particularly analyse the case where the dipolar islands reside on the bonds of a honeycomb lattice with their centres forming a kagomé array, which has been a focus of recent experimental studies.<sup>2–4,13</sup> For this kagomé array,

we find a series of regimes: firstly, the paramagnet corresponds to a gas of charges  $\pm 1$  and  $\pm 3$ . As the interaction is increased in strength, there is a crossover to a gas of charges  $\pm 1$  (kagomé ice I, K1) which terminates in an ordering transition of the charges in a two-sublattice NaCl structure on the honeycomb lattice (kagomé ice II, K2). There being exponentially many configurations of the islands which yield a NaCl charge configuration a final transition into an ordered structure with tripled unit cell removes this entropy. In a particular limit, we can extend the monopole theory for spin ice to a multipole one which captures all these regimes in analytic detail.

We supplement this by an analysis of the square ice array, where we find a hybrid Coulomb interaction between monopoles: one is the usual  $1/r$  interaction between magnetic charges, whereas the other is of entropic origin and exhibits a logarithmic distance dependence. An additional linear confining force can be removed by shifting the monopoles in the third dimension so that their locations define tetrahedra. In closing, we remark on connections to other systems as well as issues of dynamics and finite-size effects.

**Dipolar needles:** The basic degree of freedom is a dipolar island which we model with the following (idealised) properties. The magnetic moment density  $\vec{\mu}/l$  is uniform along the length,  $l$ , of the island. The islands are monodomain with the moment pointing along their axis, yielding an effective Ising spin—as was verified experimentally.<sup>1–3,13–15</sup> We take the shape of the island to be that of a needle, with a length much greater than its width, neglecting its finite transverse extent. A needle with uniform magnetisation density  $q = |\vec{\mu}|/l$  sets up the same potential  $U(\vec{R})$  as that of a pair of magnetic charges  $\pm q$  located at its tips (in the context of micromagnetic domain walls, see Refs. 16,17). The value of the Ising spin encodes which of the ends—located at  $\vec{r}_a$  and  $\vec{r}_b$ —hosts the positive charge:

$$U(\vec{R}) = \frac{\mu_0 \mu}{4\pi l} \int d\vec{l} \cdot \vec{\nabla} \frac{1}{|\vec{r} - \vec{R}|} = \frac{\mu_0 q}{4\pi} \left[ \frac{1}{|\vec{r}_a - \vec{R}|} - \frac{1}{|\vec{r}_b - \vec{R}|} \right].$$

In the following, we express lengths in units of  $a$ , the nearest-neighbor distance of the respective lattices. The dipolar islands are located on the bonds of the lattice.

In the regime  $l/a \rightarrow 1$ , which is approximately realized in recent experiments,<sup>2–4</sup> it is convenient to define  $\epsilon = 1 - l/a$ . We generally use  $q^2/a$  as the unit of energy, but shall also refer to the nearest neighbor Ising coupling strength of the islands,  $J$ , where this is more instructive.

Many of the salient features of these spin systems can be deduced intuitively in the charge picture which, in the limit of  $\epsilon \rightarrow 0$ , admits an analytic treatment.

Let us first consider the case of the kagomé array. The vertices of the kagomé lattice can have total charge  $Q = \pm 1$  (one-out, two-in or two-out, one-in) or  $Q = \pm 3$  (all in or all out). The corresponding on-site energies of  $E_1 = \frac{-2}{\sqrt{3}\epsilon a}$  and  $E_3 = \frac{2\sqrt{3}}{\epsilon a}$  are such that the latter appear only at high temperature,  $T$ , in a phase that can be classified as a paramagnet. Below  $T_{\text{ice}}^I \sim E_3 - E_1 \sim 2J$ , the population of charge  $\pm 3$  vertices is exponentially suppressed. This crossover occurs without change of symmetry. The remaining configurations with  $Q = \pm 1$  everywhere are precisely those satisfying the ice-rule (two-in, one-out or vice versa). The tendency to this kind of “order” was investigated and confirmed in recent experiments.<sup>2–4</sup>

Unlike for the case of spin-ice, where a coordination number of 4 allows for vertex charges to vanish (and finite charges are excitations in  $d = 3$ , see Ref. 12), the odd coordination of 3 enforces the presence of magnetic charges in kagomé ice at any temperature.

This kagomé ice (K1) regime is a highly frustrated phase of matter, with an entropy (known exactly) about 5/7 that of a free spin,  $S_{\text{ice}}^I \approx \frac{2}{3} \ln \frac{3}{\sqrt{2}} \approx 0.501$ .

At lower temperatures  $T_{\text{ice}}^{II} \sim q^2/a$ , interactions between vertices assert themselves. They lead to a “charge-ordered” NaCl ionic crystal, in which each sublattice of the honeycomb lattice only hosts charges  $|Q| = 1$  of a given sign—the resulting magnetic charge order is thus described by an Ising order parameter.

While the NaCl structure is fully ordered in terms of charges, it is still consistent with an exponentially large number of configurations of the underlying Ising degrees of freedom of the islands. This kagomé ice II (K2) regime is therefore only partially ordered. To calculate this entropy we map each spin configuration in kagomé ice II to a dimer covering of the hexagonal lattice: note that at any vertex, there is precisely one minority magnetic charge. As  $Q_\alpha = -Q_\beta$ , the edge with the minority charge is necessarily connected to the minority charge at the neighboring vertex, as shown in Fig. 1a). Thus, each charge configuration singles out an (oriented) dimer covering, with precisely one dimer pointing from the negative to the positive charge impinging on each vertex. The orientation of the dimers encodes the broken Ising symmetry.

The entropy of hexagonal dimer coverings is known by a mapping to the triangular Ising antiferromagnet with a well-known groundstate entropy  $S_{\text{AFM}}^\Delta$ . Adjusting for the number of elementary degrees of freedom—islands rather

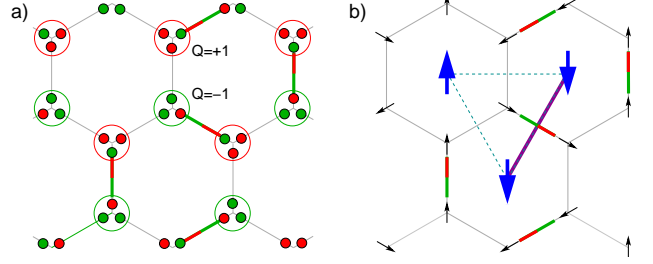


FIG. 1: (color online) a) Orientations of Ising spins on the links are mapped to a distribution of magnetic charges located at the extremities of each island. In kagomé-ice, the total charge at each vertex is constrained to  $|Q| = 1$ . At low temperatures, vertex charges order such that all vertices of sublattice  $\alpha$  have charge  $Q_\alpha = (-1)^\alpha$  (as shown). To count the configurations corresponding to that NaCl charge-state, we map these to dimer coverings of the honeycomb lattice, where oriented dimers are present at all links connecting the minority charges of the adjacent vertices. b) To count the dimer coverings of the hexagonal lattice, we note that dimers present on the hexagonal lattice can be mapped to broken links of the antiferromagnet on the dual triangular lattice. The particular configuration shown contains the unit-cell of the groundstate, formed by the three highlighted plaquettes. Arrows shown at the vertices display the direction of the local dipole moment.

then dimers—we find an entropy per island of

$$S_{\text{ice}}^{II} = \frac{1}{3} S_{\text{AFM}}^\Delta \approx 0.108. \quad (1)$$

Finally, at very low temperatures, further neighbor interactions induce a transition into an ordered phase which removes all remaining entropy. As the most favourable arrangement of a single hexagonal plaquette is for all islands to point head-to-tail,<sup>13</sup> it is natural to guess that the state should optimise the occurrence of that motif. However, no full tiling of the honeycomb lattice with such oriented loops is possible. Instead, one finds a configuration, in which 2/3 of all plaquettes are in such a state, which is precisely the one shown in Fig. 1. The three plaquettes highlighted in Fig. 1b) form the tripled  $\sqrt{3} \times \sqrt{3}$  unit-cell of the crystal with periodicity in the lattice vectors  $v_1 = (0, 3a)$  and  $v_2 = (3\sqrt{3}a/2, 3a/2)$ . We will refer to this groundstate as the ‘loop state’, below. Note that the plaquettes without an oriented loop host no dimers at all.

**Analytic magnetic multiple expansion:** The cascade of regimes outlined here can analytically be accounted for in the limit  $\epsilon \rightarrow 0$ , as each transition/crossover is associated with a parametrically different energy scale. This approach amounts to a development of a multipole expansion beyond the dumbbell model of spin ice. One finds for the energy of the loop state (expressed per hexagonal site):

$$E = \frac{q^2}{a} \left\{ \frac{-2}{\sqrt{3}\epsilon} + \left( \frac{3}{2} - \frac{\alpha}{2} \right) + \frac{3}{2}\epsilon + \left( \gamma + \frac{\delta}{4} + \frac{3}{2} \right)\epsilon^2 \right\}. \quad (2)$$

The  $\mathcal{O}(1/\epsilon)$  term enforces the  $|Q| = \pm 1$  constraint; it is due to the interactions between the charges on the same vertex. At next order, the honeycomb Madelung energy, with  $\alpha \approx 1.5422197$  drives the  $K1 \rightarrow K2$  Ising transition. This term reflects the long-range  $1/r$  interaction between the charges (monopoles) of different vertices. The  $\mathcal{O}(\epsilon^1)$  term does not distinguish between dimer configurations and hence does not lift their degeneracy; this instead happens at  $\mathcal{O}(\epsilon^2)$ , where the dipole-dipole term, with  $\gamma \approx -2.226947$ , rather than the monopole-quadrupole term with  $\delta \approx -0.5829489$ , leads to a lifting of the degeneracy between dimer states. (In passing, we note that these constants can be accurately evaluated using finite-size scaling converging as  $1/L^5$  by arranging the unit cell of the summation to have vanishing monopole, dipole and quadrupole moments).

The order of this term is easily understood. The charges  $\pm q$  are displaced a distance  $\sim \epsilon a$  from the hexagonal vertex they belong to, which generates a dipole moment of size  $|\vec{p}| \sim \epsilon a q$  and hence an interaction energy of  $\mathcal{O}(\epsilon^2)$ . This dipole moment points in one of three directions, namely along the dimer emanating from the site, so that sites connected by a dimer have aligned dipole moments. The loop pattern optimises the local dipolar energy, in that each dimer is oriented favourably with respect to its four nearest neighbours and due to the convergent nature of the  $1/r^3$  dipolar interactions in  $d = 2$ , there is little scope for this state being destabilised.

**Numerics:** Similarly, in numerics, the regimes are well resolved for small  $\epsilon$ , where they correspond to extended plateaux in thermodynamic quantities. The data shown here are for  $\epsilon = 0.05$  from Monte Carlo simulations on a lattice of linear size  $L = 24$ , with the interaction summed over periodic copies up to distance  $\Lambda = 500 L$ . We employ a mixture of single-spin flips and the short loop algorithm,<sup>18</sup> which seeks a chain of aligned spins and defines a loop when this chain first crosses itself. As the presence of different order parameters nonetheless renders a fully ergodic algorithm difficult to achieve we have pinned down the final ordering transitions by heating and cooling runs, the latter at times leading to the formation of large-scale domains.

We find a broad paramagnet  $\rightarrow$  K1 crossover, followed by a continuous and hysteresis-free onset of the Ising charge order ( $K1 \rightarrow K2$ ). These phases exhibit the predicted entropy, which drops to zero at  $T = T_{\text{order}}$ , below which we find the loop crystal, the six-fold degeneracy of which is due to the (three-fold) translational symmetry breaking, on top of the two-fold Ising spin reversal symmetry.

Interestingly, the orientation of the dipoles for a given translation of the crystal is determined in the transition at the higher temperature  $T_{\text{ice}}^{II}$ . As this ultimately determines the orientation of the loops, one could also refer to it as a chiral transition. Further, the acceptance rate of the loop moves of our Monte-Carlo simulations approaches unity in the kagomé ice K2 regime, indicating that it can be regarded as a loop gas.

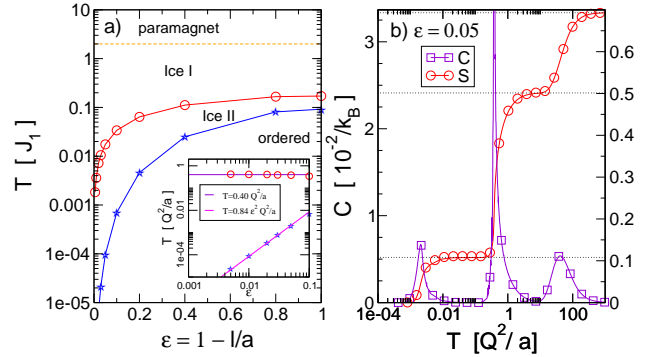


FIG. 2: (color online) Numerical results for the dipolar kagomé lattice: a) phase-diagram locating the phases (from the peaks in the heat capacity) as a function of the length of dipolar magnetic islands  $\epsilon = 1 - l/a$  and temperature in units of the NN-interaction  $J_1$ . The inset details the behaviour for small  $\epsilon$ : quadratic scaling of the ordering temperature as  $T_{\text{order}} \sim \epsilon^2 q^2/a$  as predicted by Eq. (2), and a constant transition temperature  $T_{\text{ice}}^{II} \sim q^2/a$ . b) An exemplary trace of the heat-capacity  $C$  and entropy per spin  $S$  as a function of temperature for  $\epsilon = 0.05$ . The transitions are observed as well separated peaks in the heat capacity. The entropy shows broad plateaux matching the theoretical predictions (dotted lines) for the different phases.

In Fig. 2, we show that—at small  $\epsilon$ —the temperature scales develop as predicted from the multipole expansions. However, we note that the two-peak structure of the low-temperature specific heat persists all the way to the limit  $\epsilon \rightarrow 1$  of short dipolar needles. This in particular implies that the ground state of point like Ising dipoles on the kagomé lattice with in-plane easy axes is given by the loop state.

**Magnetic monopoles in artificial spin ice:** Given the efficient description provided by the monopoles for the phase diagram of the kagomé array, it is natural to ask whether the same can be achieved for artificial (square) spin ice. Indeed, the first salient observation is that the ground state(s) of that array have zero charge on each vertex—this is possible as the local coordination is even, whereas it is odd for the kagomé array. This makes contact with Wang’s work, whose vertex types I and II correspond to  $Q = 0$  configurations. The ground state (“vacuum”) thus contains no monopoles.<sup>1,5</sup>

This leaves open the question whether monopoles nonetheless appear as effective low-energy degrees of freedom, as they do in the three-dimensional spin ice materials  $\{Dy, Ho\}_2Ti_2O_7$ . As was pointed out in Ref. 19, the short answer is no. Due to the ‘antiferromagnetic’ order in the ground state, monopoles cannot move independently as their separation leads to the creation of a costly domain wall: the monopoles remain confined.

In our previous work,<sup>5</sup> however, we have proposed a modification of the square lattice geometry consisting of introducing a height offset between islands pointing along the two different lattice directions. If this offset,  $h$ , is

chosen so that the energies of all  $Q = 0$  vertices become degenerate—as  $\epsilon \rightarrow 0$ , the endpoints of the islands then form a tetrahedron, and  $h = \epsilon/\sqrt{2}$ —the ordering disappears, and the monopoles become free to move. Indeed, their interaction is given by

$$V_Q(r) = -\frac{\mu_0}{4\pi} \frac{(2q)^2}{r}. \quad (3)$$

Even though we have an array in  $d = 2$ , the interaction follows a  $d = 3$  Coulomb law,  $1/r$ , as the field lines are not confined to the plane. However, this is not yet quite the full story. In an appropriate low-temperature setting, there is in addition an entropic interaction—which hence scales with  $T$ —between the monopoles.<sup>20,21</sup> This interaction also is of Coulomb form, but it is two-dimensional in nature, as the entropic interactions due to the fluctuations of the spin background do not know about the existence of a transverse third dimension:

$$V_s(r) \propto T \ln \left( \frac{r}{a} \right). \quad (4)$$

The strength of such a confining potential can obviously be tuned by changing the temperature—at any rate, this potential is only weak and the monopoles will look essentially free on reasonable lengthscales.

**In experiment**, this is true only in principle: a slowing-down of the dynamics makes the attainment of an equilibrium low- $T$  state difficult.<sup>1,5</sup> Indeed, the equilibration dynamics of such arrays generally becomes very sluggish when one encounters energy barriers to flipping individual islands. In the case of the kagomé array, already attaining the K2 charge-ordered crystal presents

a formidable challenge in this sense. Knowledge of the states to be expected and their order parameters should nonetheless be useful in identifying equilibration strategies, especially since a magnetic field is a versatile probe of the spin ices due to their non-collinear easy axes.<sup>22</sup>

The scheme for describing dipolar arrays in terms of magnetic monopoles, as outlined above, obviously needs to be modified when  $a\epsilon$  becomes comparable to the transverse width of the needles, set to zero at the outset. However, this will have a substantial effect only on the  $\mathcal{O}(1/\epsilon)$  term in the multipole expansion (2), and it will in particular not qualitatively change the relative sizes of the terms in the expansion in this limit.

Finally, note that the systems studied experimentally typically have a linear extent of about a few hundred islands. Given the relatively long-range of the interaction—especially that a boundary need not be (magnetic) charge neutral—this means that even the ground state may contain domain structures interesting in their own right.

*Note added in proof.* Recent work by Chern et al.<sup>23</sup> on the kagomé array obtains a phase diagram analogous to ours.

**Acknowledgements:** We are very grateful to Ravi Chandra for supplying an accurate evaluation of Eq. 2 and a careful reading of the manuscript, to him, Claudio Castelnovo and Shivaji Sondhi for collaboration on related work, and to these and Peter Schiffer, Oleg Tchernyshyov and Hartmut Zabel for useful discussions. G.M. acknowledges support from Trinity Hall Cambridge, as well as the hospitality of the University of Colorado at Boulder.

---

<sup>1</sup> R. F. Wang, C. Nisoli, R. S. Freitas, J. Li, W. McConville, B. J. Cooley, M. S. Lund, N. Samarth, C. Leighton, V. H. Crespi, and P. Schiffer, *Nature (London)* **439**, 303 (2006).

<sup>2</sup> Y. Qi, T. Brintlinger, and J. Cumings, *Phys. Rev. B* **77**, 094418 (2008).

<sup>3</sup> H. Zabel, A. Schumann, A. Westphalen, and A. Remhof, *Acta Phys. Pol. A* **115**, 59 (2009).

<sup>4</sup> M. Tanaka, E. Saitoh, H. Miyajima, T. Yamaoka, and Y. Iye, *Phys. Rev. B* **73**, 052411 (2006).

<sup>5</sup> G. Möller and R. Moessner, *Phys. Rev. Lett.* **96**, 237202 (2006).

<sup>6</sup> J. M. Luttinger and L. Tisza, *Phys. Rev.* **70**, 954 (1946).

<sup>7</sup> C. Menotti, M. Lewenstein, T. Lahaye, and T. Pfau, *AIP Conf. Proc.* **970**, 332 (2008).

<sup>8</sup> S. T. Bramwell and M. J. P. Gingras, *Science* **294**, 1495 (2001).

<sup>9</sup> A. P. Ramirez, A. Hayashi, R. J. Cava, R. Siddharthan, and B. S. Shastry, *Nature* **399**, 333 (1999).

<sup>10</sup> R. Siddharthan, B. S. Shastry, A. P. Ramirez, A. Hayashi, R. J. Cava, and S. Rosenkranz, *Phys. Rev. Lett.* **83**, 1854 (1999).

<sup>11</sup> B. C. den Hertog and M. J. P. Gingras, *Phys. Rev. Lett.* **84**, 3430 (2000).

<sup>12</sup> C. Castelnovo, R. Moessner, and S. Sondhi, *Nature* **451**, 42 (2008).

<sup>13</sup> E. Mengotti, L. J. Heyderman, A. Fraile Rodriguez, A. Bisig, L. Le Guyader, F. Nolting, and H. B. Braun, *Phys. Rev. B* **78**, 144402 (2008).

<sup>14</sup> M. Lederman, G. A. Gibson, and S. Schultz, *J. Appl. Phys.* **73**, 6961 (1993).

<sup>15</sup> S. Y. Chou, *Proc. IEEE* **85**, 652 (1997).

<sup>16</sup> E. Saitoh, H. Miyajima, T. Yamaoka, and G. Tatara, *Nature* **432**, 203 (2004).

<sup>17</sup> O. A. Tretiakov, D. Clarke, G. W. Chern, Y. B. Bazaliy, and O. Tchernyshyov, *Phys. Rev. Lett.* **100**, 127204 (2008).

<sup>18</sup> G. T. Barkema and M. E. J. Newman, *Phys. Rev. E* **57**, 1155 (1998).

<sup>19</sup> L. Mol, R. Silva, R. Silva, A. Pereira, W. Moura-Melo, and B. Costa, *J. Appl. Phys.* **106**, 063913 (2009).

<sup>20</sup> J. Kondev, *Phys. Rev. Lett.* **78**, 4320 (1997).

<sup>21</sup> R. Moessner, O. Tchernyshyov, and S. L. Sondhi, *J. Stat. Phys.* **116**, 755 (2004).

<sup>22</sup> R. Moessner, *Phys. Rev. B* **57**, R5587 (1998).

<sup>23</sup> G.-W. Chern, P. Mellado, and O. Tchernyshyov, arXiv:0906.4781 (unpublished).